

Exceptional points in the continuous spectrum of a real Hamiltonian and their manifestation as resonances.

E. Hernández^{a,*}, A. Jáuregui^b, D. Lohr^a, A. Mondragón^a

^a*Instituto de Física, Universidad Nacional Autónoma de México, Apdo. Postal 20-364, 01000 México D.F. México*

^b*Depto. de Física, Universidad de Sonora, Apdo. Postal 1626, Hermosillo, Sonora, México*

Abstract

We study the coalescence of two bound energy eigenstates embedded in the continuous spectrum of a real pseudo-Hermitian Hamiltonian of von Neumann-Wigner type and the exceptional point produced by this coalescence. At the exceptional point, the two unnormalized Jost eigenfunctions are no longer linearly independent but coalesce to give rise to a Jordan cycle of generalized bound state eigenfunctions embedded in the continuum and a Jordan block representation of the Hamiltonian. The time evolution of the regular scattering function is unitary, while the time evolution of the generalized eigenfunctions is pseudounitary. We disturb the potential $V[4]$ by means of a truncation, this perturbation breaks the exceptional point in two resonances, the phase shift shows a jump of magnitude 2π and the shape of the cross section shows two inverted peaks, this behaviour is due to the interference between the two resonances and the background.

Keywords: Singularity theory, Scattering theory, Phases: geometric; dynamics or topological

PACS: 02.40.Xx, 03.65.Nk, 03.65.Vf

1. Introduction

In recent years the development and progress of quantum physics with non-Hermitian operators has given rise to important accomplishments in dif-

*Corresponding author

Email address: queta@fisica.unam.mx (E. Hernández)

ferent fields [1, 2, 3, 4, 5, 6, 7, 8, 9], and in particular in the study of the physics of exceptional points [2, 7, 10, 11, 12, 13]. Exceptional points appear as a coalescence of both the eigenvalue and eigenfunction of a Hamiltonian of a given quantum system [14]. Exceptional points are often found in non-Hermitian Hamiltonian matrices of finite dimension [2, 7, 13, 15, 16, 17, 18] or in Hermitian Hamiltonians with non-selfadjoint boundary conditions [19, 20], in both cases they depend on a set of control parameters. Many theoretical [13, 15, 16, 17, 21, 22, 23, 24, 25, 26, 27, 28, 29] and experimental [30, 31, 32, 33, 34, 35, 36] works are related to exceptional points produced by an accidental degeneracy of resonant states. An interesting study of exceptional points was done by O. Atabek et. al., who have shown that by tuning the laser parameters, i.e. intensity and wavelength, it is possible to produce the coalescence of two Floquet resonances, which describe the photodissociation of the Na_2 and H_2^+ molecules. Accidental degeneracy of these resonances lead to an exceptional point in the parameter space of the system[37].

Exceptional points in the real and continuous spectrum of a Hamiltonian of infinite dimension [38, 39, 40, 41] have received much less attention than the case of non-Hermitian Hamiltonians of finite dimension. These exceptional points are associated with bound states embedded in the continuous energy of scattering states. Bound states embedded in the continuous energy were first proposed by von Neumann and Wigner in 1929 [42]. They showed that certain spatially oscillating potentials could support a bound state with energy above the potential barrier. Later Stillinger et. al. [43] proposed that these states could be found in certain atomic and molecular systems, and in ultra-thin layer structures of semiconductors. They showed [44] that lattices could be used to construct potentials that support bound states with positive energies. J. Pappademos et. al. [45] showed that with methods of supersymmetric quantum mechanics one can construct potentials supporting bound states in the continuum. A.A. Stahlhofen [46] constructed local potentials with positive eigenvalues for the one-dimensional Schrödinger equation. A possible way to observe a bound state embedded in the continuum is by perturbing the potential. T. A. Weber and D. L. Pursey [47] studied the s -wave scattering by a von Neumann-Wigner type potential and showed that by truncating the potential the bound state in the continuum manifest itself as a resonance. A great number of examples of potentials that support a bound state in the continuum have been studied [48]. The first experimental evidence of these states was reported by F. Capasso et. al. [49] in a super

lattice consisting of thin superconducting layers of AlInAs/GaInAs. Bound states embedded in the continuum have been recently observed in optical wave guide arrays [50, 51, 52].

The first observation of a bound state associated with an exceptional point (defect modes) in PT-symmetric optical lattice was done by A. Regensburger et. al. [53]. Some theoretical research about the formation of defect modes have been done in the framework of PT-symmetric optics [41, 53, 54, 55, 56]. S. Longhi showed that exceptional points in the continuum can appear in non-Hermitian optical lattices with engineered defects, using a two times iterated discrete Darboux transformation [41].

The Darboux transformation method is a powerful technique for the generation of bound states in the continuum associated with exceptional points and it allows an analytical study of the degeneracy of the eigenvalues and eigenfunctions of the Hamiltonian $H[4]$. The main objective of this paper is to clarify some physical and mathematical properties of an exceptional point that is obtained from the coalescence of two exceptional points in the real continuous energy spectrum of a pseudo-Hermitian Hamiltonian $H[4]$ with a real potential of von Neumann-Wigner type. This potential is generated from the eigenfunctions of a free particle Hamiltonian by means of a four times iterated Darboux transformation when the transformation functions are degenerated in the continuum [57]. Although this potential is obtained without reference to any specific field forces, it can be used as an approximant to a more realistic potential.

This paper is organized as follows: In section 2 we generate a Hamiltonian $H[4]$ by means of a four times iterated and completely degenerated Darboux transformation. In section 3 we compute the Jost solutions of $H[4]$ normalized to unit probability flux at infinity and we show that at $k = \pm q$, the Wronskian of the two unnormalized Jost solutions of $H[4]$ vanishes, this property identifies these points as exceptional points in the spectrum of the Hamiltonian $H[4]$. Section 4 is devoted to show that at the exceptional points the Hamiltonian $H[4]$ has a Jordan block matrix representation and a Jordan cycle of generalized eigenfunctions. In section 5 we show that the regular scattering solution vanishes at exceptional points $k = \pm q$. In section 6 we show that the presence of an exceptional point in the spectrum of $H[4]$ does not alter the unitary evolution of the regular time dependent wave function. In section 7 we show the pseudounitary time evolution of the generalized eigenfunction. In section 8 we perturb the potential $V[4]$ with a cut off at a finite value $r = a$, and show that the exceptional points manifest themselves

as two resonances. In section 9 we study the interference between the two resonances and the background term, which comes from an infinite number of zeros of the Jost function. A summary of the main results and conclusions are presented in section 10.

2. The Hamiltonian $H[4]$

A Hamiltonian that has two exceptional points in its real and continuous spectrum may be generated by means of a four times iterated and completely degenerated Darboux transformation [40].

The potential $V[4]$ obtained from the four times iterated Darboux transformation should not have any singularities that are not present in the initial potential; this condition puts constraints on the potential $V[4]$ that fix the number of free parameters as it will be shown in this section.

The radial Schrödinger equation is

$$H[4]\psi(r) = k^2\psi(r), \quad (1)$$

and the Hamiltonian is

$$H[4] = -\frac{\partial^2}{\partial r^2} + V[4], \quad (2)$$

with units $2m = 1$ and $\hbar = 1$.

The radial Schrödinger equation is defined in $[0, \infty)$ and we will compute the regular scattering solutions that satisfy the boundary condition $\psi(0) = 0$.

According with Crum's generalization of the Darboux theorem [58], the function

$$\psi(r) = \frac{W(\phi, \partial_q \phi, \partial_q^2 \phi, \partial_q^3 \phi, e^{\pm ikr})}{W(\phi, \partial_q \phi, \partial_q^2 \phi, \partial_q^3 \phi)}, \quad (3)$$

is an eigenfunction of the radial Schrödinger equation with the potential

$$V[4] = V_0 - 2\frac{d^2}{dr^2} \ln W(\phi, \partial_q \phi, \partial_q^2 \phi, \partial_q^3 \phi). \quad (4)$$

In these expressions, $W(\phi, \dots, \partial_q^3 \phi)$ is the Wronskian of the transformation function $\phi(q, r)$ and its first derivatives with respect to q , and $W(\phi, \dots, e^{\pm ikr})$ is the Wronskian of the transformation function, its first three derivatives with respect to q and $e^{\pm ikr}$, which is an eigenfunction of the free particle radial Hamiltonian with eigenvalue $E = k^2$. The transformation function is

also an eigenfunction of the free particle radial Hamiltonian with eigenvalue $E = q^2$

$$\phi(q, r) = \sin(qr + \delta(q)), \quad (5)$$

and $\partial_q \phi$ is shorthand for $\partial \phi / \partial q$. The phase shift $\delta(q)$ in the right side of eq.(5) is a smooth function of the wave number q .

The Wronskian $W(\phi, \partial_q \phi, \partial_q^2 \phi, \partial_q^3 \phi) \equiv W_1(q, r)$ is readily computed from (5) and the potential $V[4]$ is obtained from $W_1(q, r)$ and its derivatives with respect to r ,

$$V[4] = -2 \frac{1}{W_1^2(q, r)} \left(W_1''(q, r) W_1(q, r) - W_1'^2(q, r) \right), \quad (6)$$

the prime means differentiation with respect to r .

An explicit expression for $W_1(q, r)$ is the following

$$\begin{aligned} W_1(q, r) &= 16(q\gamma)^4 - 12(q\gamma)^2 + 8(q^3\gamma_2)(q\gamma) - 12(q^2\gamma_1)^2 \\ &+ 24[(q^2\gamma_1)(q\gamma) + (q\gamma)^2] \cos 2\theta + 3 \sin^2 2\theta \\ &+ [16(q\gamma)^3 - 12q\gamma - 12q^2\gamma_1 - 4q^3\gamma_2] \sin 2\theta, \end{aligned} \quad (7)$$

where

$$\begin{aligned} \theta(r) &= qr + \delta(q), \gamma(r) = \partial_q \theta = r + \gamma_0, \gamma_0 = \partial_q \delta(q), \\ \gamma_1 &= \partial_q^2 \delta(q), \gamma_2 = \partial_q^3 \delta(q). \end{aligned} \quad (8)$$

For large values of r , the dominant term in the right hand side of eq.(7) is $(q\gamma)^4$ which is positive and grows with r as r^4 . Hence, for large values of r , $W_1(q, r)$ is a positive and increasing function of r . However, if the phase $\delta(q)$ is left unconstrained, $W_1(q, r)$ could take a negative value at the origin of the radial coordinate ($r = 0$), in which case it should vanish for some positive value of r , giving rise to a singularity of the potential $V[4]$ at that point.

In the case under consideration, the necessary condition for the validity of the method of the Darboux transformation means that the Wronskian $W_1(q, r)$ should not vanish for any positive value of r . Therefore, to avoid the appearance of singularities in $V[4]$ at positive values of r , we will set the condition

$$W_1(q, 0) > 0, \quad (9)$$

which defines the phase shift $\delta(q)$, and from equation (8) the value of the functions γ_0 , γ_1 , and γ_2 is computed. An explicit demonstration is given in Appendix A.

From equation (A.10), we verify that the Wronskian $W_1(q, r)$, for $r = 0$, is given by

$$W_1(q, 0) = \frac{12\beta^2}{(1 + (\alpha q - \beta)^2)^2}, \quad (10)$$

where α and β are two parameters that determine the potential $V[4]$. However, the resulting expression for $V[4]$ is too long and not very illustrative. A graphical representation of $V[4]$ as a function of r is shown in figure 1, where we used values of α and β so that the potential supports a bound state in the continuum in $q = 1$; this particular restriction for the parameters will be shown in section 4.

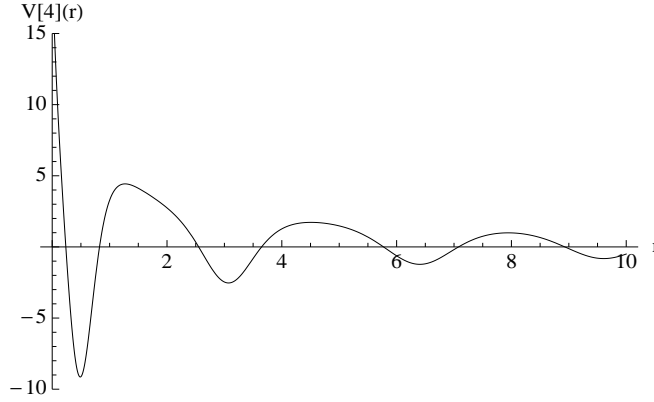


Figure 1: This graph shows the potential $V[4]$ for the values of the parameters $\alpha = 1$, $\beta = 3$ fixed at $q = 1$.

The asymptotic behaviour of $W_1(q, r)$ for large values of r is determined by the term $(q\gamma)^4$ which grows as r^4 and is the dominant term in the right hand side of equation (7), with this result and equation (6), we get

$$V[4] = 8q \frac{\sin 2(qr + \delta(q))}{r} + O(r^{-2}), \quad (11)$$

then, $V[4]$ is a potential of von Neumann-Wigner type [42].

3. The Jost solutions and the exceptional points in the spectrum of $H[4]$

The two linearly independent unnormalized Jost solutions of $H[4]$, that belong to the energy eigenvalues $E = k^2$ and behave as outgoing and incom-

ing waves for large values of r , are given in eq.(3). Notice that all terms in the last column of the Wronskian $W(\phi, \dots, \partial_q^3 \phi, e^{\pm ikr})$ are proportional to $e^{\pm ikr}$. Hence, the unnormalized Jost solutions take the form

$$f^\pm(k, r) = \frac{1}{W_1(q, r)} w^\pm(k, r) e^{\pm ikr}, \quad (12)$$

where the function $w^\pm(k, r)$ is the reduced Wronskian defined as

$$w^\pm(k, r) e^{\pm ikr} = W(\phi, \dots, \partial_q^3 \phi, e^{\pm ikr}). \quad (13)$$

From this definition, it follows that $w^\pm(k, r)$ is a complex function of its arguments

$$w^\pm(k, r) = u(k, r) \pm iv(k, r). \quad (14)$$

Explicit expressions for the functions $u(k, r)$ and $v(k, r)$ are given by

$$\begin{aligned} u(k, r) = & 16q^4 (k^2 - q^2)^2 \gamma^4 - 12q^2 (k^4 + 6q^2 k^2 + q^4) \gamma^2 \\ & + 8\gamma_2 q^4 (k^2 - q^2)^2 \gamma - 12\gamma_1^2 q^4 (k^2 - q^2)^2 \\ & + 24q^2 [(k^4 - 4q^2 k^2 - q^4) \gamma^2 + q\gamma_1 (k^4 - q^4) \gamma] \\ & \times \cos 2\theta + [16q^3 (k^4 - q^4) \gamma^3 \\ & - 12q (k^4 - 4q^2 k^2 - q^4) \gamma - 4\gamma_2 q^3 (k^4 - q^4) \\ & - 12\gamma_1 q^2 (k^4 - 4q^2 k^2 - q^4)] \sin 2\theta \\ & + 3 (k^4 + 6q^2 k^2 + q^4) \sin^2 2\theta, \end{aligned} \quad (15)$$

and

$$\begin{aligned} v(k, r) = & 64q^4 k (k^2 - q^2) \gamma^3 - 24q^2 k (k^2 + q^2) \gamma \\ & + 8\gamma_2 q^4 k (k^2 - q^2) - 48\gamma_1 q^5 k + [32q^4 k \\ & \times (k^2 - q^2) \gamma^3 + 24q^2 k (k^2 + q^2) \gamma - 8\gamma_2 q^4 k \\ & \times (k^2 - q^2) + 48\gamma_1 q^5 k] \cos 2\theta + [96q^5 k \gamma^2 \\ & - 48\gamma_1 q^4 k (k^2 - q^2) \gamma - 12q k (k^2 + q^2)] \sin 2\theta \\ & + 6q k (k^2 + q^2) \sin 4\theta. \end{aligned} \quad (16)$$

For large values of r , the asymptotic behaviour of $w^\pm(k, r)$ is dominated by the highest power of r . From eqs.(14), (15) and (16) we get

$$w^\pm(k, r) = 16(k^2 - q^2)^2 (qr)^4 [1 + O(r^{-1})], \quad (17)$$

and from eq.(A.10) we get

$$W_1(q, r) = 16(qr)^4[1 + O(r^{-1})], \quad (18)$$

hence, for large values of r the unnormalized Jost solutions are given by

$$f^\pm(k, r) = (k^2 - q^2)^2[1 + O(r^{-1})]e^{\pm ikr}. \quad (19)$$

at infinity the Jost solutions are incoming and outgoing waves, at the origin they have a finite value [59]. The factor $(k^2 - q^2)^2$ is the flux of probability current at infinity of the unnormalized Jost solutions. Therefore, the Jost solutions of $H[4]$ normalized to unit probability flux at infinity are

$$F^\pm(k, r) = \frac{f^\pm(k, r)}{(k^2 - q^2)^2} = \frac{1}{(k^2 - q^2)^2} \frac{w^\pm(k, r)}{W_1(q, r)} e^{\pm ikr}, \quad k^2 \neq q^2. \quad (20)$$

Each pair of linearly independent Jost solutions belongs to a point $E_k = k^2$, with $k^2 \neq q^2$, in the spectrum of $H[4]$.

The Wronskian of the unnormalized Jost solutions is readily computed from (12) and eqs.(14)-(16)

$$W(f^+(k, r), f^-(k, r)) = -2ik(k^2 - q^2)^4. \quad (21)$$

At the points $k = \pm q$, the Wronskian of the two unnormalized Jost solutions of $H[4]$ vanishes, then the two unnormalized Jost solutions are no longer linearly independent and coalesce in the function

$$\begin{aligned} f^\pm(q, r) &= 4q^2 \frac{24q^2}{W_1(q, r)} [-2q^2 \gamma^2 \cos \theta \\ &+ (q\gamma + q^2 \gamma_1) \sin \theta + \sin^2 \theta \cos \theta] e^{\mp i\delta}, \end{aligned} \quad (22)$$

which is obtained from eq.(12) when $k = \pm q$. From the asymptotic behaviour of $W_1(q, r)$ it follows the function $f^\pm(q, r)$ can be normalized and therefore is a bound state eigenfunction embedded in the continuum.

The property given in eq.(21) identifies the points $k = \pm q$ as exceptional points in the spectrum of the Hamiltonian $H[4]$. This property is a manifestation that the Hamiltonian $H[4]$ is a real non-selfadjoint Hamiltonian.

The Wronskian of the unnormalized Jost solutions, eq.(21), goes to zero as the fourth power of $(k - q)$ as a result of the coalescence of two functions to form the exceptional point. The exceptional points are an obstruction of

a complete biorthonormal system of eigenfunctions of a Hamiltonian operator and its adjoint [1].

These exceptional points are associated with a double pole in the normalization factor of the Jost eigenfunctions $F^\pm(k, r)$, see equation (20), but they are not associated with a double pole in the scattering matrix. The scattering matrix and the cross section are regular analytical functions of the wave number k [40]. Hence, the presence of the exceptional points is not associated with a structure in the cross section as it is in the case with the coalescence of two resonant states, where the cross section shows a splitting peak [19, 20].

4. Jordan cycle of generalized eigenfunctions and Jordan block representation of $H[4]$

The normalized Jost solutions of $H[4]$, as functions of the wave number k , may be written as the sum of a singular and a regular part [40]

$$\begin{aligned} F^\pm(k, r) = & \frac{\psi_B(q, r)e^{\mp i\delta(q)}}{(k-q)^2} + \frac{\chi_B^\pm(q, r)e^{\mp i\delta(q)}}{(k-q)} + \frac{\psi_B(-q, r)e^{\pm i\delta(q)}}{(k+q)^2} \\ & + \frac{\chi_B^\pm(-q, r)e^{\pm i\delta(q)}}{(k+q)} + h^\pm(k, r). \end{aligned} \quad (23)$$

Explicit expressions for the functions $\psi_B(q, r)$ and $\chi_B^\pm(q, r)$ as functions of r , are

$$\psi_B(q, r) = \frac{24q^2}{W_1(q, r)}[-2q^2\gamma^2 \cos \theta + (q\gamma + q^2\gamma_1) \sin \theta + \sin^2 \theta \cos \theta] \quad (24)$$

and

$$\chi_B^\pm(q, r) = \chi_B(q, r) \mp i\gamma_0\psi_B(q, r), \quad (25)$$

where

$$\begin{aligned} \chi_B(q, r) = & \frac{8q}{W_1(q, r)}[-2q^3\gamma^3 \sin \theta - 3q^2\gamma^2 \cos \theta + 3q\gamma \sin^3 \theta \\ & - \gamma_2 q^3 \sin \theta + 3\gamma_1 \gamma q^3 \cos \theta + 3 \sin^2 \theta \cos \theta]. \end{aligned} \quad (26)$$

The functions γ_0, γ_1 and γ_2 are given in equations (A.9). The condition $\beta = 3\alpha q$ assures that $\psi_B(q, 0) = 0$. For the exceptional point at $k = -q$, this condition implies a change of sign in the β parameter.

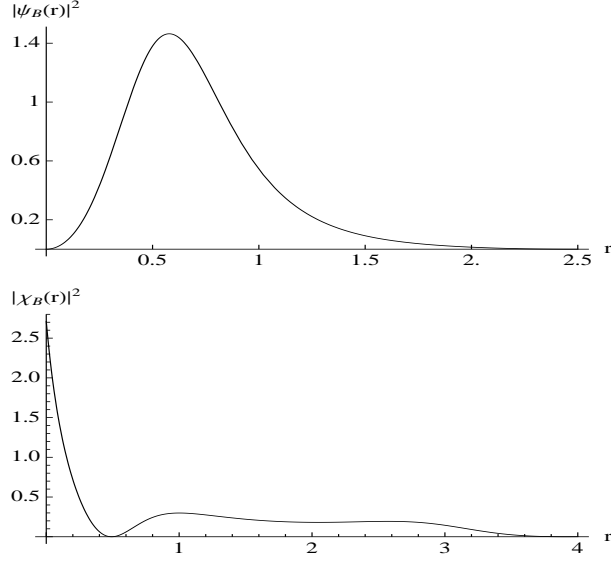


Figure 2: This graph shows the normalized bound state eigenfunction $\psi_B(q, r)$ and the generalized eigenfunction $\chi_B(q, r)$ as function of r computed for $q = 1$ and the values of the parameters $\alpha = 1$ and $\beta = 3$.

The functions $\psi_B(q, r)$ and $\chi_B(q, r)$ are the elements of a Jordan cycle of generalized eigenfunctions of the Hamiltonian that belong to the same point $k = q$ in its spectrum, and satisfy the set of coupled equations

$$H[4]\psi_B(q, r) = q^2\psi_B(q, r) \quad (27)$$

and

$$H[4]\chi_B(q, r) = q^2\chi_B(q, r) + 2q\psi_B(q, r). \quad (28)$$

$\psi_B(q, r)$ represents the bound state eigenfunction embedded in the continuum and $\chi_B(q, r)$ is a generalized eigenfunction of $H[4]$. This Jordan cycle of generalized eigenfunctions is associated with a Jordan block representation of the Hamiltonian $H[4]$. This property is made evident if the equations (27) and (28) are written in matrix form

$$\begin{bmatrix} H[4] \mathbf{1}_{2 \times 2} \end{bmatrix} \Psi_B(q, r) = \mathcal{H}_B(q) \Psi_B(q, r), \quad (29)$$

where

$$\Psi_B(q, r) = \begin{pmatrix} \psi_B(q, r) \\ \chi_B(q, r) \end{pmatrix} \quad \text{and} \quad \mathcal{H}_B(q) = \begin{pmatrix} q^2 & 0 \\ 2q & q^2 \end{pmatrix}. \quad (30)$$

From (29), it is evident that the matrix $\mathcal{H}_B(q)$ is a matrix representation of the Hamiltonian $H[4]$ in the two dimensional functional space spanned by the generalized eigenfunctions $\{\psi_B(q, r), \chi_B(q, r)\}$.

This space is a subset of the rigged Hilbert space of continuous, complex functions of the variables (q, r) with continuous first and second derivatives with respect to r , with r in the semi-infinite straight line $0 \leq r < \infty$. Therefore, the two dimensional subspace of functions spanned by the generalized eigenfunctions $\{\psi_B(q, r), \chi_B(q, r)\}$ is in the domain of $H[4]$.

The matrix $\mathcal{H}_B(q)$ is a Jordan block of 2×2 [61] and can not be brought to diagonal form by means of a similarity transformation with a unitary matrix [62].

The real non-symmetric matrix $\mathcal{H}_B(q)$ is η -pseudo-Hermitian [63]

$$\mathcal{H}_B^\dagger(q) = \eta^{-1} \mathcal{H}_B(q) \eta, \quad (31)$$

with

$$\eta = \begin{pmatrix} 0 & 1 \\ 1 & 0 \end{pmatrix}. \quad (32)$$

Hence, the Hamiltonian operator $H[4]$ when acting on the functional space spanned by the generalized eigenfunctions $\{\psi_B(q, r), \chi_B(q, r)\}$ is also η -pseudo-Hermitian.

In the figure 2 we show the graphical representation of the generalized eigenfunctions $\psi_B(q, r)$ and $\chi_B(q, r)$ as function of r .

The unnormalized probability amplitude of the eigenfunction $\psi_B(q, r)$, as a function of r , for the parameters of the potential $V[4]$ is shown in figure 3. The bound state is formed in the first well of oscillatory potential for energy $E_q = q^2 = 1$.

5. Scattering solutions

In this section it will be shown that the regular scattering solution $\psi_s(k, r)$ vanishes at exceptional points $k = \pm q$.

The regular scattering solution of $H[4]$ is given by [59]

$$\psi_s(k, r) = \frac{i}{2} \left[F^-(k, r) - S(k) F^+(k, r) \right], \quad k \neq q, \quad (33)$$

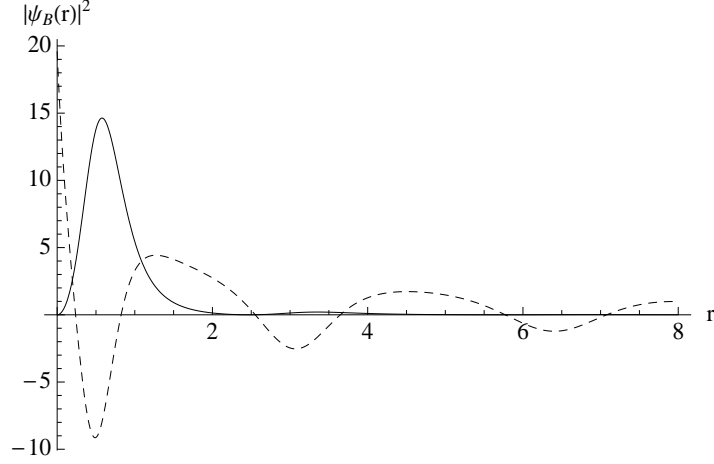


Figure 3: The graph shows with a continuous line the unnormalized probability amplitude of the bound state solution as a function of r for the values of the parameters in the potential $V[4]$ and $q = 1.0$. The dashed line represents the potential $V[4]$.

where the scattering matrix $S(k)$ is

$$S(k) = \frac{F^-(k, 0)}{F^+(k, 0)}. \quad (34)$$

The regular scattering solution $\psi_s(k, r)$ is written in terms of the regular solution $\Phi(k, r)$ as

$$\psi_s(k, r) = k(k^2 - q^2)^2 \frac{\Phi(k, r)}{f^+(k, 0)}, \quad (35)$$

where $f^+(k, 0)$ is the unnormalized Jost function evaluated at $r = 0$ and it is a continuous function of the wave number k .

The regular solution $\Phi(k, r)$ is defined as [59]

$$\Phi(k, r) = \frac{i}{2k} [F^+(k, 0)F^-(k, r) - F^-(k, 0)F^+(k, r)]. \quad (36)$$

From the definition of the Jost solutions, eq.(20), we get for the regular solution

$$\Phi(k, r) = \frac{i}{2k} \frac{1}{(k^2 - q^2)^4} \frac{1}{W_1(q, 0)W_1(q, r)}$$

$$\times \left[w^+(k, 0)w^-(k, r)e^{-ikr} - w^-(k, 0)w^+(k, r)e^{ikr} \right]. \quad (37)$$

In order to make explicit the behaviour of $\Phi(k, r)$ at the neighbourhood of $k = q$, we expand the bracket term

$$\phi(k, r) = w^+(k, 0)w^-(k, r)e^{-ikr} - w^-(k, 0)w^+(k, r)e^{ikr} \quad (38)$$

in a Taylor series as a function of k . Computing the derivatives of $\phi(k, r)$, with help of the explicit expressions of $w^\pm(k, r)$ given in eqs.(14), (15) and (16), we get

$$\phi(k, r) \Big|_{k=q} = \frac{d\phi(k, r)}{dk} \Big|_{k=q} = \frac{d^2\phi(k, r)}{dk^2} \Big|_{k=q} = \frac{d^3\phi(k, r)}{dk^3} \Big|_{k=q} = 0, \quad (39)$$

therefore the function $\phi(k, r)$ can be written as

$$\phi(k, r) = \frac{1}{4!} \frac{d^4\phi(k, r)}{dk^4} \Big|_{k=q} (k - q)^4 + O((k - q)^5). \quad (40)$$

Substitution of eq.(40) in eq.(37) gives for the regular solution at the neighbourhood of $k = q$,

$$\Phi(k, r) = \frac{i}{2k} \frac{1}{(k + q)^4} \frac{1}{W_1(q, 0)W_1(q, r)} \left[\frac{1}{4!} \frac{d^4\phi(k, r)}{dk^4} \Big|_{k=q} + O((k - q)) \right]. \quad (41)$$

At the exceptional point $k = q$ the regular solution $\Phi(k, r)$ is a finite function

$$\Phi(q, r) = \frac{i}{4!2^5q^5} \frac{1}{W_1(q, 0)W_1(q, r)} \frac{d^4\phi(k, r)}{dk^4} \Big|_{k=q}. \quad (42)$$

Therefore, from eq.(35), at the exceptional point the regular scattering solution vanishes,

$$\psi_s(q, r) = 0. \quad (43)$$

The vanishing of the regular scattering solution at the exceptional point $k = q$ does not have consequences for the physical observables such as the phase shift $\delta(k)$ and the cross section $\sigma(k)$.

From (14) and (20) the explicit expression for the regular scattering solution is

$$\psi_s(k, r) = \frac{1}{(k^2 - q^2)^2} \frac{e^{i\Delta(k)}}{W_1(q, r)} [u(k, r) \sin(kr + \Delta(k))]$$

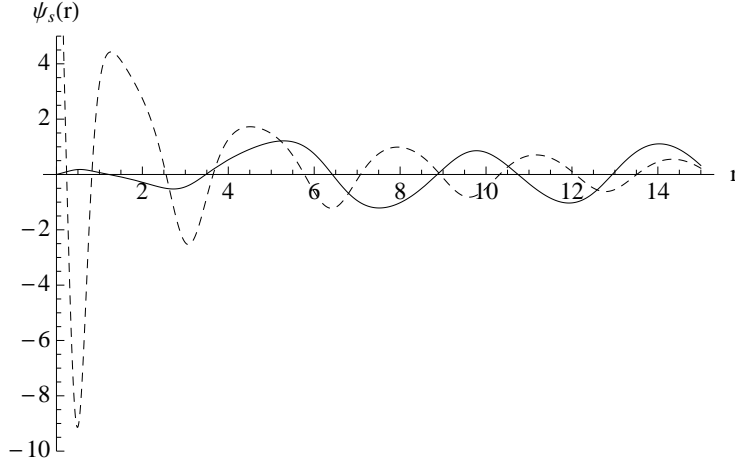


Figure 4: The graph shows with a continuous line the regular scattering solution as a function of r for the values of the parameters in the potential $V[4]$ and $k = 1.5$. The dashed line is the potential $V[4]$.

$$+ v(k, r) \cos(kr + \Delta(k))], \quad (44)$$

where $\Delta(k)$ is the phase shift

$$\Delta(k) = -\arctan \frac{v(k, 0)}{u(k, 0)}. \quad (45)$$

A graphical representation of the regular scattering solution is shown in figure 4. As the value of k approaches q the amplitude of the oscillations decreases.

6. Unitary time evolution of the regular scattering solutions of $H[4]$

The regular time dependent wave function built as a linear combination of the regular scattering solutions of $H[4]$ is

$$\Psi_r(r, t) = \int C(k) e^{-ik^2(t-t_0)} \psi_s(k, r) dk. \quad (46)$$

This is a solution of the time dependent Schrödinger equation

$$i \frac{\partial \Psi_r(r, t)}{\partial t} = H[4] \Psi_r(r, t), \quad (47)$$

as it may be verified by substitution of (46) in (47).

The coefficient $C(k)$ occurring in the right hand side of eq.(46) is a quadratically integrable function of k .

Since the regular scattering solutions vanishes at the exceptional point it does not contribute to the integral in the right hand side of eq.(46).

Therefore, the presence of an exceptional point in the spectrum of $H[4]$ does not alter the unitary evolution of the regular time dependent wave function.

7. Pseudounitary time evolution of the generalized eigenfunctions

The two generalized eigenfunctions $\psi_B(q, r)$ and $\chi_B(q, r)$ belong to the same spectral point, $E_q = q^2$; in consequence, they evolve in time together. Hence, it should be convenient to introduce a matrix notation to deal with the two together,

$$\Psi(r, t) = C(q, t)\Psi_B(q, r), \quad (48)$$

where $\Psi_B(q, r)$ is the two component vector of the doublet, defined in eq.(30), and $C(q, t)$ is the 2×2 matrix of time dependent coefficient of the wave functions $\psi_B(q, r)$ and $\chi_B(q, r)$.

Substitution of $\Psi(r, t)$ in the time dependent Schrödinger equation gives the following set of coupled equations written in matrix form

$$i\frac{\partial C(q, t)}{\partial t}\Psi_B(q, r) = C(q, t)H[4]\mathbf{1}_{2 \times 2}\Psi_B(q, r) = C(q, t)\mathcal{H}_B(q)\Psi_B(q, r), \quad (49)$$

making abstraction of $\Psi_B(q, r)$, we obtain

$$i\frac{\partial C(q, t)}{\partial t} = C(q, t)\mathcal{H}_B(q), \quad (50)$$

where $\mathcal{H}_B(q)$ is given by eq.(30).

Integrating eq.(50) we get

$$C(q, t) = e^{-i\mathcal{H}_B(q)t}, \quad (51)$$

writing $\mathcal{H}_B(q)$ in explicit form in (51), and computing the exponential, we obtain

$$C(q, t) = e^{-iq^2t} \begin{pmatrix} 1 & 0 \\ -i2qt & 1 \end{pmatrix}. \quad (52)$$

Substitution of the expressions (52) and (30) in (48) gives the evolve in time of the two generalized components of the doublet $\Psi(r, t)$

$$\psi_B(r, t) = e^{-iq^2 t} \psi_B(q, r) \quad (53)$$

and

$$\chi_B(r, t) = e^{-iq^2 t} \chi_B(q, r) - i2qt e^{-iq^2 t} \psi_B(q, r). \quad (54)$$

The component $\psi_B(r, t)$, describing the time evolution of the bound state eigenfunction embedded in the continuum, exhibits a unitary evolution in time, while the component $\chi_B(r, t)$ has a linear growth with time. This behaviour is a direct consequence of the pseudounitariness of the Hamiltonian at $E_q = q^2$. Therefore, the wave function $\Psi(r, t)$ and its norm will grow linearly with time t . This type of behaviour has been found by Longhi et. al. [41] in a non-Hermitian Hamiltonian.

8. Truncated $V[4]$ potential

The bound state in the continuum associated with an exceptional point presented in this paper is not related to the poles of the scattering matrix and, therefore, is not possible to perform a direct measurement. However, this state is very fragile and any small disturbance can break the equilibrium necessary for its formation, thus showing the presence of the exceptional point [47]. In this section we disturb the potential by cutting off its range at a value $r = a$. A cut off value of $a = 5000$ means that the perturbation is very small; however, it is enough to show the breaking of the bound state in the continuum into two resonances.

The Schrödinger equation is

$$\left[-\frac{d^2}{dr^2} + V(r) \right] \varphi(k, r) = k^2 \varphi(k, r), \quad (55)$$

where

$$V(r) = \begin{cases} V[4](r) & r \leq a \\ 0 & r > a \end{cases} \quad (56)$$

and $\varphi(k, r)$ satisfies the boundary condition $\varphi(k, 0) = 0$.

The solution in both regions are given by

$$\varphi(k, r) = A \begin{cases} \psi_s(k, r) & r \leq a \\ \frac{1}{2ik} [G(k)e^{ikr} - F(k)e^{-ikr}] & r > a \end{cases} \quad (57)$$

where $F(k)$ is the Jost function of the perturbed problem. From the continuity condition of the function $\varphi(k, r)$ and its derivative at $r = a$ we get

$$F(k) = e^{ika} [\psi'_s(k, a) - ik\psi_s(k, a)], \quad (58)$$

and

$$G(k) = e^{-ika} [\psi'_s(k, a) + ik\psi_s(k, a)], \quad (59)$$

where the prime means differentiation with respect to r .

From eq.(44) the derivative of the regular scattering solution is

$$\begin{aligned} \psi'_s(k, r) &= \frac{1}{(k^2 - q^2)^2} \frac{e^{i\Delta(k)}}{W_1^2(q, r)} \{ -W_1'(q, r) [u(k, r) \\ &\times \sin(kr + \Delta(k)) + v(k, r) \cos(kr + \Delta(k))] \\ &+ W_1(q, r) [(u'(k, r) - kv(k, r)) \sin(kr + \Delta(k)) \\ &+ (v'(k, r) + ku(k, r)) \cos(kr + \Delta(k))] \}. \end{aligned} \quad (60)$$

Substituting (44) and (60) in (58) we get for the Jost function the expression:

$$F(k) = \frac{1}{(k^2 - q^2)^2} \frac{e^{i(ka + \Delta(k))}}{W_1^2(q, r)} [d(k) + ig(k)], \quad (61)$$

and for the function $G(k)$

$$G(k) = \frac{1}{(k^2 - q^2)^2} \frac{e^{-i(ka - \Delta(k))}}{W_1^2(q, r)} [d(k) - ig(k)], \quad (62)$$

with

$$\begin{aligned} d(k) &= \left[u'(k, a)W_1(q, a) - u(k, a)W_1'(q, a) - kv(k, a)W_1(q, a) \right] \\ &\times \sin(ka + \Delta(k)) + \left[v'(k, a)W_1(q, a) - v(k, a)W_1'(q, a) \right. \\ &\left. + ku(k, a)W_1(q, a) \right] \cos(ka + \Delta(k)), \end{aligned} \quad (63)$$

and

$$g(k) = -kW_1(q, a) [u(k, a) \sin(ka + \Delta(k)) + v(k, a) \cos(ka + \Delta(k))]. \quad (64)$$

The scattering matrix $S(k)$ is given by:

$$S(k) = \frac{G(k)}{F(k)}. \quad (65)$$

The zeros of the Jost function $F(k)$ are the poles of $S(k)$. With substitution of (61) and (62) in (65), $S(k)$ is written as

$$S(k) = \frac{e^{-ika} [d(k) - ig(k)]}{e^{ika} [d(k) + ig(k)]}. \quad (66)$$

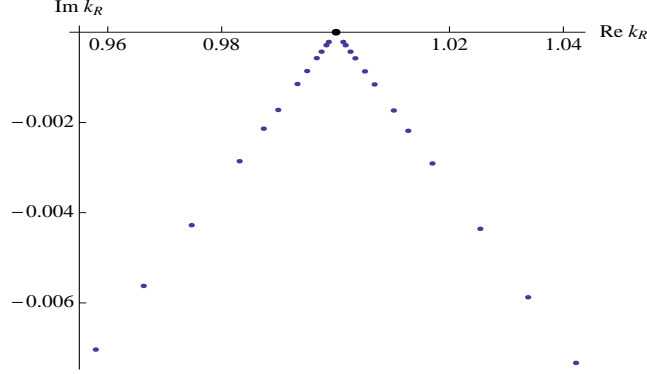


Figure 5: The trajectory of the resonances in the complex k -plane for several values of the cut off parameter. The point on the real axis represents the exceptional point.

From the equation (66) the poles of the $S(k)$ matrix, in the neighbourhood of the exceptional point $k = q$, are obtained from the equation

$$d(k) + ig(k) = 0. \quad (67)$$

We solved numerically this equation for different values of the cut off parameter a and found two zeros of the Jost function in the fourth quadrant of the complex k -plane close to $q = 1$, which correspond to the resonances that came from the exceptional point. There are other zeros of the Jost function near the real axis of the k -plane; however, by changing the value of cut off parameter they do not lead to the exceptional point. In figure 5 we show the trajectory of the resonances in the complex k -plane as a result of the numerical solutions of equation (67), for the values of the parameters $\alpha = 1$, $\beta = 3$, $q = 1$ and several values of the cut off parameter a in the range $120 - 5000$. As the cut off parameter increases, the two resonances approach the real axis to coalesce in the exceptional point.

In figure 6 we show the unnormalized probability amplitudes of the Gamow functions corresponding to two resonant states for the parameter values

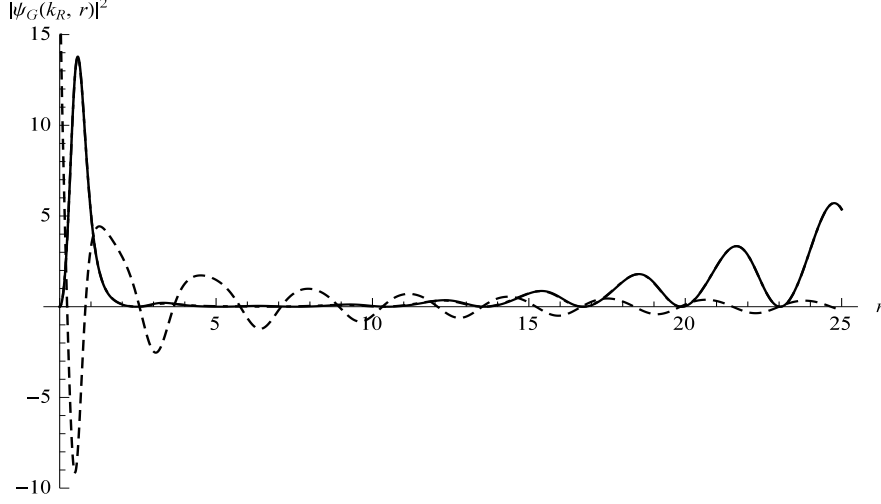


Figure 6: The probability amplitude of the Gamow functions as a function of r for the parameters $\alpha = 1$, $\beta = 3$ and the cut off $a = 5000$. The dashed line is the perturbed potential $V(r)$. The dot-dashed line represents the Gamow functions for the resonances $k_1 = 0.9989844032 - i0.0001730065$. The continuous line represents the Gamow functions for the resonance $k_2 = 1.0010155756 - i0.0001731296$.

of the perturbed potential with $a = 5000$ and resonance wave numbers $k_1 = 0.9989844032$, $\Gamma_1/2 = 0.0001730065$ and $k_2 = 1.0010155756$, $\Gamma_2/2 = 0.0001731296$. In order to show the probability amplitude of the Gamow functions and the perturbed potential on the same scale, we plot the unnormalized solutions. The resonances coming from the breaking of the exceptional point are formed in the first well of the potential. The resonances are very close to the real axis, as seen in figure 5, therefore the probability amplitude of the Gamow functions corresponding to each resonance are almost indistinguishable in figure 6.

The scattering matrix $S(k)$ given in eq. (66) is written as:

$$S(k) = e^{2i\delta_a(k)}, \quad (68)$$

where

$$\delta_a(k) = -\arctan \frac{d(k) \sin ka + g(k) \cos ka}{d(k) \cos ka - g(k) \sin ka}, \quad (69)$$

is the phase shift of the perturbed potential.

In figure 7 we show the phase shift $\delta_a(k)$ as a function of the wave number k , and its behaviour in the neighbourhood of $k = 1$ for the cut off parameter

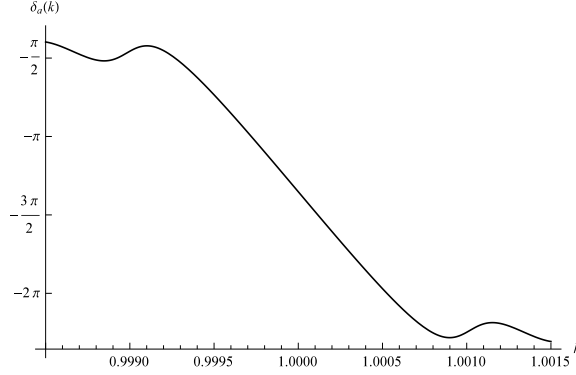


Figure 7: Phase shift $\delta(k)$ as a function of the wave number k for $q = 1$ and the parameters $\alpha = 1$, $\beta = 3$ and the cut off $a = 5000$.

$a = 5000$, where it shows a jump of 2π , characteristic of the case where there are two very close resonances [19]. The jump starts near $-\pi/2$ and ends near $-5\pi/2$.

The cross section is defined as

$$\sigma(k) = \frac{4\pi}{k^2} \sin^2 \delta_a(k). \quad (70)$$

The figure 8 shows the cross section as a function of the wave number k . The two inverted peaks, where it vanishes, are a result of the phase shift passing through the values $-\pi$ and -2π , where $\sigma(k)$ is minimum; whereas the peak around $k = 1.0001$ is due to $\delta_a(k)$ passing through $-3\pi/2$, where $\sigma(k)$ is maximum.

9. Interference of two close resonances

In this section we will show that the shape of the two inverted peaks of the cross section $\sigma(k)$, obtained in the previous section, is due to the interference of the two resonances and the background.

When the first and second absolute moments of the potential exist, and the potential decreases at infinity faster than any exponential or if it vanishes identically beyond a finite radius, the Jost function $F(k)$ is an entire function of k [59]. The entire function of k , $F(k)$ may be written in a form of an infinite product of zeros according to Hadamard's form of the Weierstrass

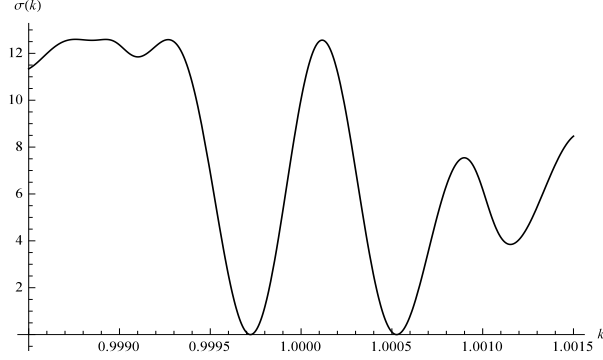


Figure 8: Cross section $\sigma(k)$ as a function of the wave number k , for $q = 1$, and for the cut off $a = 5000$, and the values of the parameters $\alpha = 1$, $\beta = 3$.

factorization theorem [64] and, by using a theorem of Pfluger [65],

$$F(k) = F(0) \exp(ikR) \prod_{n=1}^{\infty} \left(1 - \frac{k}{k_n}\right) \quad (71)$$

where R is the range of the potential, $F(0) = Ak$ with A a constant and $\{k_n\}$ are the zeros of $F(k)$ [59].

In order to show the interference of the two resonances and the background we write the Jost function $F(k)$ in the explicit form of a product of two zeros

$$F(k) = \left(k - k_1 + i\frac{\Gamma_1}{2}\right) \left(k - k_2 + i\frac{\Gamma_2}{2}\right) \exp(ika) D(k), \quad (72)$$

where the product $\exp(ika) D(k)$ correspond to the background component of the Jost function with

$$D(k) = F(0) \frac{1}{(k_1 - i\frac{\Gamma_1}{2})(k_2 - i\frac{\Gamma_2}{2})} \prod_{n=3}^{\infty} \left(1 - \frac{k}{k_n}\right). \quad (73)$$

We consider a small perturbation of the potential by taking a large value of the cut off parameter a . This guarantees that the doublet of isolated resonances is close to the real axis of the complex k -plane. Furthermore we assume that the other zeros of $F(k)$, contained in $D(k)$, correspond to more

far resonances, and thus the infinite product of zeros on the right hand side of equation (73) has a smooth behaviour of k , which can be written as

$$D(k) = \mu(k)(1 + i\lambda(k)), \quad (74)$$

where $\mu(k)$ and $\lambda(k)$ are real and smooth functions of k . From eqs.(72), (73) and (74), the Jost function takes the form

$$\begin{aligned} F(k) &= \mu(k) \{ (\Upsilon(k) - \lambda(k)Z(k)) \cos ka - (\lambda(k)\Upsilon(k) + Z(k)) \sin ka \\ &+ i[(\Upsilon(k) - \lambda(k)Z(k)) \sin ka + (\lambda(k)\Upsilon(k) + Z(k)) \cos ka] \}, \end{aligned} \quad (75)$$

where

$$\Upsilon(k) = (k - k_1)(k - k_2) - \frac{\Gamma_1 \Gamma_2}{4}, \quad (76)$$

$$Z(k) = \frac{1}{2}[(k - k_1)\Gamma_2 + (k - k_2)\Gamma_1]. \quad (77)$$

The Jost function is written in terms of the phase shift as

$$F(k) = |F(k)|e^{-i\delta(k)}, \quad (78)$$

and the phase shift is given by

$$\delta(k) = -\arctan \frac{(\Upsilon(k) - \lambda(k)Z(k)) \sin ka + (\lambda(k)\Upsilon(k) + Z(k)) \cos ka}{(\Upsilon(k) - \lambda(k)Z(k)) \cos ka - (\lambda(k)\Upsilon(k) + Z(k)) \sin ka}. \quad (79)$$

The cross section $\sigma(k)$ is given by the expression

$$\sigma(k) = \frac{4\pi}{k^2} \frac{1}{1 + \lambda^2(k)} \frac{[(\Upsilon(k) - \lambda(k)Z(k)) \sin ka + (\lambda(k)\Upsilon(k) + Z(k)) \cos ka]^2}{\Upsilon^2(k) + Z^2(k)}. \quad (80)$$

From the obtained expressions for the phase shift and the cross section we can see that the function $\lambda(k)$ gives a measure of the interference between the two resonances due to the background term.

For the computation of the cross section $\sigma(k)$ of the approximation given by eq.(80), we take the resonance wave numbers obtained from the numerical calculation of the Jost function zeros eq.(67) for a cut off parameter $a = 5000$

$$k_1 = 0.9989844032, \quad \Gamma_1/2 = 0.0001730065 \quad (81)$$

$$k_2 = 1.0010155756, \quad \Gamma_2/2 = 0.0001731296 \quad (82)$$

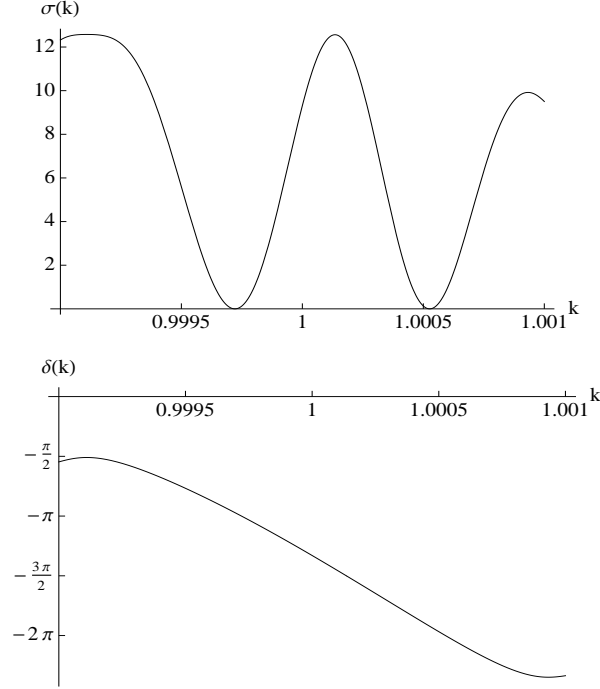


Figure 9: The cross section $\sigma(k)$ and the phase shift $\delta(k)$ as function of k , calculated for the values of the resonances $k_1 = 0.9989844032$, $\Gamma_1/2 = 0.0001730065$, $k_2 = 1.0010155756$, $\Gamma_2/2 = 0.0001731296$, and the mixing parameters $\lambda_0 = 1311.3931$, $\lambda_1 = -1312.2167$ and a cut off $a = 5000$.

The assumption of the resonances being well isolated allow us to parametrise the function $\lambda(k)$ as a linear polynomial of k ,

$$\lambda(k) = \lambda_0 + \lambda_1 k, \quad (83)$$

the parameter values $\lambda_0 = 1311.3931$ and $\lambda_1 = -1312.2167$ are obtained from to fit the minima of the approximated cross section to the minima of the exact cross section.

After the substitution of $\lambda(k)$ at eq.(79), the phase shift $\delta(k)$ in the neighbourhood of the two resonances exhibits a value near $-\pi/2$ and then the known jump of 2π , as can be seen from the graph for the phase shift in the lower part of the figure 9. This displacement of the phase shift is due to the interference between the two resonance and the non-resonant background term contained in the $\lambda(k)$ function. In the upper part of figure 9 we

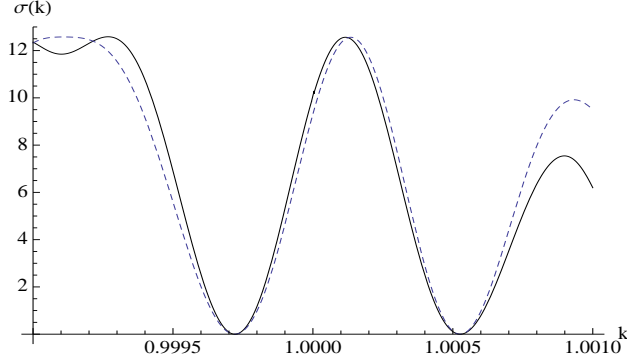


Figure 10: The cross section $\sigma(k)$, as function of k . The continuous line is the numerically exact calculation, equation (70), for the parameter values $\alpha = 1$, $\beta = 3$, $q = 1$, and the cut off parameter $a = 5000$, the dashed line is the cross section of the approximation given by equation (80), calculated for the values of the resonances $k_1 = 0.9989844032$, $\Gamma_1/2 = 0.0001730065$, $k_2 = 1.0010155756$, $\Gamma_2/2 = 0.0001731296$, and the mixing parameters $\lambda_0 = 1311.3931$, $\lambda_1 = -1312.2167$.

show the cross section as function of k , it has the same resonant structure as the exact cross section. This resonant structure is a manifestation of the Ramsauer-Townsend effect [59, 60].

Figure 10 shows the comparison of the results for the cross section, as a function of the wave number k , obtained from the numerically exact calculation with eq.(70) and the results computed with the approximation given by eq.(80) in the neighbourhood of the resonances. The fit to the cross section using the approximation of eq.(80) is pretty good, it reproduces the shape of the resonant structure shown in the exact calculation and allows us to give an explanation of this phenomenon in the neighbourhood of the two resonances.

10. Summary and conclusions

An example of exceptional points in the continuous spectrum of a real, pseudo-Hermitian Hamiltonian $H[4]$ of von Neumann-Wigner type is presented and discussed. The Hamiltonian $H[4]$ and the free particle Hamiltonian H_0 are isospectral. In the general case, to each point in this continuous spectrum correspond two linearly independent Jost solutions which behave at infinity as incoming and outgoing waves. However, here we have shown that in the continuous spectrum of $H[4]$ there are two exceptional points at wave numbers $k = \pm q$, these exceptional points are associated with a double pole in

the normalization factor of the Jost eigenfunctions normalized to unit flux at infinity. At the exceptional points, the two unnormalized Jost eigenfunctions are no longer linearly independent and coalesce to give rise to Jordan cycles of length two of generalized quadratically integrable bound states eigenfunctions embedded in the continuum and a Jordan block representation of the Hamiltonian $H[4]$. The bound state embedded in the continuum is formed in the first well of the potential $V[4]$. The scattering eigenfunction vanishes at the exceptional point, in consequence, the time evolution of the regular scattering function is unitary. The generalized eigenfunctions $\psi_B(q, r)$ and $\chi_B(q, r)$ evolve in time together. The component $\psi_B(r, t)$ describing the bound state eigenfunction embedded in the continuum has an unitary evolution in time, while the component $\chi_B(r, t)$ has a linear growth with time; therefore the time evolution of the generalized eigenfunctions is pseudounitary. The scattering matrix $S(k)$ is a regular function of k at the exceptional points, that is, the Jordan cycle of generalized bound states eigenfunctions of $H[4]$ in the continuum is not associated with a pole of the scattering matrix. The perturbation of the potential $V[4]$, with a cut off value $r = a$, manifests the exceptional points as two resonant states in the complex k -plane. The two resonances are formed in the first well of the perturbed potential. The phase shift shows a jump of magnitude 2π and the cross section shows two inverted peaks, where it vanishes, for the values of k where the phase shift is $-\pi$ and -2π ; and it has a local maximum at the value of k where the phase shift is $-3\pi/2$. The shape of the cross section with two inverted peaks in the neighbourhood of $k = q$ is due to the interference between the two resonances when interacting with the background.

Acknowledgements

We would like to thank Prof. E. Ley Koo (IF-UNAM) for some interesting discussions on the problem. This work was partially supported by CONACyT México under Contract No. 132059, DGAPA-UNAM Contract No. PAPIIT:IN113712 and DCEN-UNISON.

Appendix A. Computation of the Wronskian $W_1(k, r)$

In this appendix we compute the explicit expression for the Wronskian $W_1(q, r)$.

From eqs. (7) and (8) we have

$$\begin{aligned}
W_1(q, 0) &= 16 \left(q \frac{d\delta(q)}{dq} \right)^4 - 12 \left(q \frac{d\delta(q)}{dq} \right)^2 + 8 \left(q^3 \frac{d^3\delta(q)}{dq^3} \right) \\
&\times \left(q \frac{d\delta(q)}{dq} \right) - 12 \left(q^2 \frac{d^2\delta(q)}{dq^2} \right)^2 + 24 \left[\left(q^2 \frac{d^2\delta(q)}{dq^2} \right) \right. \\
&\times \left. \left(q \frac{d\delta(q)}{dq} \right) + \left(q \frac{d\delta(q)}{dq} \right)^2 \right] \cos 2\delta(q) \\
&+ 3 \sin^2 2\delta(q) + \left[16 \left(q \frac{d\delta(q)}{dq} \right)^3 - 12 \left(q \frac{d\delta(q)}{dq} \right) \right. \\
&\times \left. \left(q^2 \frac{d^2\delta(q)}{dq^2} \right) - 4 \left(q^3 \frac{d^3\delta(q)}{dq^3} \right) \right] \sin 2\delta(q). \tag{A.1}
\end{aligned}$$

To simplify the notation, we define a new function $t(q)$ as

$$t(q) := \tan \delta(q), \tag{A.2}$$

then

$$\sin 2\delta(q) = \frac{2t(q)}{1+t^2(q)} \quad \text{and} \quad \cos 2\delta(q) = \frac{1-t^2(q)}{1+t^2(q)}. \tag{A.3}$$

Written in terms of $t(q)$, eq.(A.1) takes the form

$$\begin{aligned}
W_1(q, 0) &= \frac{4 \left(-t(q) + q t_q(q) \right)}{\left(1 + t^2(q) \right)^2} \left[3 \left(-t(q) + q t_q(q) \right) + 6 q^2 t_{qq}(q) \right. \\
&\times \left. \left(-t(q) + q t_q(q) \right) + 2 q^3 t_{qqq}(q) \right] - 3 q^4 \left(\frac{d}{dq} \left(-t(q) + q t_q(q) \right) \right)^2, \tag{A.4}
\end{aligned}$$

in this expression t_q is shorthand for dt/dq .

Now it is evident from (A.4) that if $t(q)$ satisfies

$$-t(q) + q t_q(q) = \beta, \tag{A.5}$$

the equation (A.4) becomes an identity and the condition given in (9) is satisfied provided that

$$W_1(q, 0) = \frac{12\beta^2}{(1+t^2(q))^2}. \tag{A.6}$$

Integrating (A.5) we get

$$t(q) = \alpha q - \beta, \quad (\text{A.7})$$

and according to equation (A.2)

$$\delta(q) = \arctan(\alpha q - \beta), \quad (\text{A.8})$$

in these expressions α and β are free parameters, but $\beta \neq 0$.

Once the phase shift $\delta(q)$ is known as an explicit function of q , the functions γ_0 , γ_1 and γ_2 are obtained from its first, second and third derivative, respectively,

$$\begin{aligned} \gamma_0 &= \frac{\alpha}{1 + (\alpha q - \beta)^2}, \quad \gamma_1 = -\frac{2\alpha^2(\alpha q - \beta)}{(1 + (\alpha q - \beta)^2)^2}, \\ \gamma_2 &= -\frac{2\alpha^3(1 - 3(\alpha q - \beta)^2)}{(1 + (\alpha q - \beta)^2)^3}. \end{aligned} \quad (\text{A.9})$$

With the help of these expressions and equation (7) we get for $W_1(q, r)$ the following expression

$$\begin{aligned} W_1(q, r) &= \frac{12\beta^2}{(1 + (\alpha q - \beta)^2)^2} + \frac{24\beta\alpha q}{(1 + (\alpha q - \beta)^2)^2} \\ &\times (\cos 2qr - 1) + \frac{12\alpha q((\alpha q)^2 + \beta^2 - 1)}{(1 + (\alpha q - \beta)^2)^2} \sin 2qr \\ &+ 16[(qr)^4 + \frac{4\alpha q}{(1 + (\alpha q - \beta)^2)}(qr)^3 \\ &+ \frac{6(\alpha q)^2}{(1 + (\alpha q - \beta)^2)^2}(qr)^2 + \frac{3(\alpha q)^3}{(1 + (\alpha q - \beta)^2)^2} \\ &\times (qr)] - 12 \left[(qr)^2 + \frac{2\alpha q}{(1 + (\alpha q - \beta)^2)}(qr) \right] \\ &+ 24 \left[(qr)^2 + \frac{2\alpha q(1 - \beta(\alpha q - \beta))}{(1 + (\alpha q - \beta)^2)^2}(qr) \right] \\ &\times \cos 2(qr + \delta(q)) + \left[16((qr)^3 \right. \\ &+ \frac{3\alpha q}{(1 + (\alpha q - \beta)^2)}(qr)^2 + \frac{3(\alpha q)^2}{(1 + (\alpha q - \beta)^2)^2} \\ &\times (qr) \left. \right] - 12(qr) \sin 2(qr + \delta(q)) \\ &+ 3 \left[\frac{1 - 6(\alpha q - \beta)^2 + (\alpha q - \beta)^4}{(1 + (\alpha q - \beta)^2)^2} \right] \end{aligned}$$

$$\begin{aligned} & \times \sin^2 2qr + \frac{4(\alpha q - \beta)(1 - (\alpha q - \beta)^2)}{(1 + (\alpha q - \beta)^2)^2} \\ & \times \sin 2qr \cos 2qr \Big]. \end{aligned} \tag{A.10}$$

References

References

- [1] N. Moiseyev, Non-Hermitian Quantum Mechanics, Cambridge University Press, Cambridge, 2011.
- [2] C. Bender, A. Fring, U. Günther, H. Jones, J. Phys. A: Math. Theor. 45 (2012) 440301.
- [3] C. M. Bender, Rep. Prog. Phys. 70 (2007) 947.
- [4] F. Bagarello, J.-P. Gazeau, F. H. Szafraniec and M. Znojil, Non-Selfadjoint Operators in Quantum Physics: Mathematical Aspects, Wiley, 2015.
- [5] E. Narevicius and N. Moiseyev, Phys. Rev. Lett. 84 (2000) 1681 .
- [6] N. Moiseyev, S. Scheit and L. S. Cederbaum, J. Chem. Phys. 121 (2004) 722.
- [7] M. V. Berry, Czech. J. Phys. 54 (2004) 1039.
- [8] I. Rotter, J. Phys. A: Math. Theor. 42 (2009) 153001.
- [9] D. C. Brody, J. Phys. A: Math. Theor. 47 (2014) 035305.
- [10] W. D. Heiss, Czech. J. Phys. 54 (2004) 1091.
- [11] U. Günther, I. Rotter, and B. F. Samsonov, J. Phys. A: Math. Theor. 40 (2007) 8815.
- [12] W. D. Heiss, J. Phys. A: Math. Theor. 45 (2012) 444016.
- [13] W. D. Heiss, J. Phys. A: Math. Gen. 37 (2004) 2455.
- [14] T. Kato, Perturbation Theory for Linear Operators, Springer, Berlin, 2013.

- [15] O. Félix-Beltrán, M. Gómez-Bock, E. Hernández, A. Mondragón and M. Mondragón, *Int. J. Theor. Phys.* 50 (2011) 2291.
- [16] R. Lefebvre and N. Moiseyev, *J. Phys B: At. Mol. Opt. Phys.* 43 (2010) 095401.
- [17] H. Cartarius, J. Main and G. Wunner, *Phys. Rev. A* 79 (2009) 053408.
- [18] H. Estrada, L. S. Cederbaum and W. Domcke, *J. Chem. Phys.* 84 (1986) 152.
- [19] E. Hernández, A. Jáuregui and A. Mondragón, *J. Phys. A: Math. Theor.* 33 (2000) 4507.
- [20] E. Hernández, A. Jáuregui and A. Mondragón, *Phys. Rev. E* **84** (2011) 046209; *J. Phys. A: Math. Gen.* 39 (2006) 10087.
- [21] O. Latinne, N. J. Kylstra, M. Dörr, J. Purvis, M. Terao-Dunseath, C. J. Joachain, P. G. Burke and C. J. Noble, *Phys. Rev. Lett.* 74 (1995) 46.
- [22] H.-X. Cui, X.-W. Cao, M. Kang, T.-F. Li, M. Yang, T.-J. Guo, Q.-H. Guo and J. Cheng, *Optics Express* 21 (2013) 13368.
- [23] S. Cavalli and D. De Fazio, *Theor. Chem. Acc.* 129 (2011) 141.
- [24] H. J. Korsch and S. Mossmann, *J. Phys. A: Math. Gen.* 36 (2003) 2139.
- [25] R. Lefebvre, O. Atabek, M. Sindelka and N. Moiseyev, *Phys. Rev. Lett.* 103 (2009) 123003.
- [26] J. Okolowicz and M. Płoszajczak, *Phys. Rev. C* 80 (2009) 034619.
- [27] H. Cartarius, J. Main and G. Wunner, *Phys. Rev. A* 77 (2008) 013618; H. Cartarius and N. Moiseyev, *Phys. Rev. A* 84 (2011) 013419.
- [28] I. Gilary, A. A. Mailybaev and N. Moiseyev, *Phys. Rev. A* 88 (2013) 010102(R).
- [29] D. J. Kalita, and A. K. Gupta, *J. Chem. Phys.* 137 (2012) 214315.
- [30] P. von Brentano and M. Philipp, *Phys. Lett. B* 454 (1999) 171.

- [31] M. Philipp, P. von Brentano, G. Pascovici, A. Richter, Phys. Rev. E 62 (2000) 1922.
- [32] C. Dembowski, H.-D. Gräf, H. L. Harney, A. Heine, W. D. Heiss, H. Rehfeld and A. Richter, Phys. Rev. Lett. 86 (2001) 787.
- [33] C. Dembowski, B. Dietz, H.-D. Gräf, H. L. Harney, A. Heine, W. D. Heiss and A. Richter, Phys. Rev. Lett. 90 (2003) 034101.
- [34] S.-B. Lee, J. Yang, S. Moon, S.-Y. Lee, J.-B. Shim, S. W. Kim, J.-H. Lee and K. An, Phys. Rev. Lett. 103 (2009) 134101.
- [35] T. Stehmann, W. D. Heiss and F. G. Scholtz, J. Phys. A: Math. Gen. 37 (2004) 7813.
- [36] B. Dietz, T. Friedrich, J. Metz, M. Miski-Oglu, A. Richter, F. Schäfer and C. A. Stafford, Phys. Rev. E 75 (2007) 027201; B. Dietz, H. L. Harney, O. N. Kirillov, M. Miski-Oglu, A. Richter and F. Schäfer, Phys. Rev. Lett. 106 (2011) 150403.
- [37] O. Atabek, R. Lefebvre, M. Lepers, A. Jaouadi, O. Dulieu and V. Kokoouline, Phys. Rev. Lett. 106 (2011) 173002; A. Jaouadi, M. Desouter-Lecomte, R. Lefebvre and O. Atabek, J. Phys. B: At. Mol. Opt. Phys. 46 (2013) 145402; R. Lefebvre, O. Atabek, M. Šindelka and N. Moiseyev, Phys. Rev. Lett. 103 (2009) 123003.
- [38] A. A. Andrianov, and A. V. Sokolov, SIGMA 7, 111 (2011); A. V. Sokolov, SIGMA 7 (2011) 112.
- [39] A. V. Sokolov, A. A. Andrianov, and F. Cannata, J. Phys. A: Math. Gen. 39 (2006) 10207.
- [40] N. Fernández-García, E. Hernández, A. Jáuregui, and A. Mondragón, J. Phys. A: Math. Theor. 46 (2013) 175302.
- [41] S. Longhi and G. Della Valle, Phys. Rev. A **89** (2014) 052132; S. Longhi, Opt. Lett. 39 (2014) 1697.
- [42] J. von Neumann and E. P. Wigner, Z. Physik 30 (1929) 465.
- [43] F. H. Stillinger and T. A. Weber, Phys. Rev. A 10 (1974) 1122.

- [44] F. H. Stillinger and D. R. Herrick, Phys. Rev. A **11** (1975) 446.
- [45] J. Pappademos, U. Sukhatme and A. Pagnamenta, Phys. Rev. A **48** (1993) 3525.
- [46] A. A. Stahlhofen, Phys. Rev. A **51** (1995) 934; A. A. Stahlhofen, J. Phys. A: Math. Gen. **29** (1996) L581.
- [47] T. A. Weber and D. L. Pursey, Phys. Rev. A **57** (1998) 3534.
- [48] M. S. P. Eastham and H. Kalf, Schrödinger type Operators with Continuous Spectra, Pitman, London, 1982.
- [49] F. Capasso, C. Sirtori, J. Faist, D. L. Sivco, S.-G. Chu and A. Y. Cho, Nature **358** (1992) 565.
- [50] Y. Plotnik, O. Peleg, F. Dreisow, M. Heinrich, S. Nolte, A. Szameit and M. Segev, Phys. Rev. Lett. **107** (2011) 183901.
- [51] S. Weimann, Y. Xu, R. Keil, A. E. Miroshnichenko, A. Tünnermann, S. Nolte, A. A. Sukhorukov, A. Szameit and Y. S. Kivshar, Phys. Rev. Lett. **111** (2013) 240403.
- [52] G. Corrielli, G. Della Valle, A. Crespi, R. Osellame and S. Longhi, Phys. Rev. Lett. **111** (2013) 220403.
- [53] A. Regensburger, M. A. Miri, C. Bersch, J. Näger, G. Onishchukov, D. N. Christodoulides and U. Peschel, Phys. Rev. Lett. **110** (2013) 223902.
- [54] K. Zhou, Z. Guo, J. Wang and S. Liu, Opt. Lett. **35** (2010) 2928.
- [55] M. I. Molina and Y. S. Kivshar, Stud. Appl. Math. **133** (2014) 337.
- [56] X.-F. Zhu, Opt. Exp. **23** (2015) 22274.
- [57] V. B. Matveev and M. A. Salle, Darboux Transformations and Solitons, Springer, Berlin, 1991.
- [58] M. M. Crum, Q. J. Math. **6** (1955) 121.
- [59] R. G. Newton, Chapter 12 Scattering Theory of Waves and Particles, Springer, Berlin, 2014.

- [60] S. Weinberg, Chapter 3 The Quantum Theory of Fields, Cambridge University Press, Cambridge, 1995.
- [61] E. Hernández, A. Jáuregui, and A. Mondragón, Phys. Rev. A 67 (2003) 022721.
- [62] P. Lancaster and M. Tismenetsky, The Theory of Matrices, Academic Press, New York, 1985.
- [63] A. Mostafazadeh, Int. J. Geom. Methods Mod. Phys. 7 (2010) 1191.
- [64] R. P. Boas, Entire functions, Academic Press, New York, 1954, p. 22.
- [65] A. Pfluger, Commun. Math. Helv. 16 (1943) 1 .